

P.C. Guess<sup>1,2\*</sup>, Y. Zhang<sup>2</sup>, J.-W. Kim<sup>2</sup>,  
E.D. Rekow<sup>3</sup>, and V.P. Thompson<sup>2</sup>

<sup>1</sup>Department of Prosthodontics, Albert-Ludwigs-University, Freiburg, Germany; <sup>2</sup>Department of Biomaterials and Biomimetics, New York University College of Dentistry, 345 East 24th Street, New York, NY 10010, USA; and <sup>3</sup>Office of the Provost, New York University, New York, NY, USA; \*corresponding author, [petra.guess@uniklinik-freiburg.de](mailto:petra.guess@uniklinik-freiburg.de)

*J Dent Res* 89(6):592-596, 2010

## ABSTRACT

Zirconia-based restorations are widely used in prosthetic dentistry, but their susceptibility to post-sintering cementation surface treatments remains controversial. We hypothesized that grinding (600-grit) and alumina abrasion (50  $\mu\text{m}$ , 5 sec, 0.5 MPa) affect the damage modes and reliability of zirconia core material. Monolithic CAD/CAM-machined and sintered Y-TZP plates (0.5 mm thickness) were adhesively cemented to dentin-like composite substrates. Uni-axial mouth-motion cyclic contact was applied through a tungsten carbide spherical indenter ( $r = 3.18$  mm). Results showed that zirconia core ceramic is vulnerable to lower surface radial fracture after grinding or alumina abrasion, while the as-received control chiefly fractured from load-application surface cone fracture. Significantly lower reliability of ground and alumina-abraded compared with the as-received zirconia core ceramic can be attributed to damage induced on the cementation surface. Clinical relevance concerning surface treatment protocols for zirconia framework materials prior to cementation is addressed.

**KEY WORDS:** zirconia framework, surface treatment, fatigue reliability, radial fracture, cone fracture.

DOI: 10.1177/0022034510363253

Received February 11, 2009; Last revision December 29, 2009; Accepted January 8, 2010

# Damage and Reliability of Y-TZP after Cementation Surface Treatment

## INTRODUCTION

Yttria-stabilized tetragonal zirconia polycrystal (Y-TZP) applied as a framework material has been used increasingly in restorative and implant dentistry. Compared with other all-ceramic systems, Y-TZP exhibits superior mechanical properties, owing to a transformation toughening mechanism (Christel *et al.*, 1989). Despite the high flexural strength (900 to 1200 MPa) (Tinschert *et al.*, 2000; Filser *et al.*, 2001) and fracture toughness (6 to 10 MPa  $\text{m}^{1/2}$ ) (Christel *et al.*, 1989), short- to mid-term clinical studies revealed Y-TZP framework fractures in extended fixed partial dentures (FPDs) (Sailer *et al.*, 2007; Taskonak *et al.*, 2008) and crown restorations (Aboushelib *et al.*, 2008). The clinical failure of all-ceramic restorations is a complex combination of factors, including restoration geometry and damage caused by processing and handling procedures, as well as by cyclic loading from occlusal function.

Final adjustments of the cementation surface of a Y-TZP framework by grinding and polishing to achieve better restoration fit are commonly performed by dental technicians and practitioners (Aboushelib *et al.*, 2008). Airborne particle abrasion for the Y-TZP cementation surface is widely recommended to increase micromechanical retention and durability of resin bonding (Wolfart *et al.*, 2007). The influence of these procedures on the long-term stability of Y-TZP frameworks is not fully understood.

Reported results on the strength and reliability of Y-TZP ceramics after various surface treatments differ, depending on the degree of induced surface damage (Luthardt *et al.*, 2002, 2004; Zhang *et al.*, 2004; Curtis *et al.*, 2006) and on stress-induced surface damage as well as grain size and amount of stabilizer (Kosmac *et al.*, 1999, 2000; Guazzato *et al.*, 2005; Curtis *et al.*, 2006). Classic ceramic failure theory has shown the existence of competing damage modes under load (Lawn *et al.*, 2001). In addition to strength-related flexural radial cracks, cone cracks may originate from the surface from concentrated contact stresses during cyclic loading (Kim *et al.*, 2007) (Fig. 1). Therefore, there is a need for systematic investigation of fatigue damage and the reliability of Y-TZP core ceramic subjected to clinically relevant post-sintering surface treatments.

The aim of the present study was to investigate the effects of 2 routinely used post-sintering cementation surface modification techniques, namely, grinding and alumina abrasion, on the performance of Y-TZP layers on composite substrates. Contact-induced damage and failure mechanism of Y-TZP dental ceramic under cyclic Hertzian contact loading as well as reliability were investigated in a flat-layer model. Control tests were conducted on as-received CAD/CAM-machined specimens on composite substrates.

## MATERIALS & METHODS

CAD/CAM zirconia plates (12 x 12 x 0.8 mm, n = 72) were manufactured from pre-sintered Y-TZP blocks (IPS e.max ZirCAD; Ivoclar Vivadent, Schaan, Liechtenstein; composition according to manufacturer in wt%, ZrO<sub>2</sub>, 87.0-95.0%; Y<sub>2</sub>O<sub>3</sub>, 4.0-6.0%; HfO<sub>2</sub>, 1.0-5.0%; and Al<sub>2</sub>O<sub>3</sub>, 0.1-1.0%; grain size, 0.50-0.65 μm) with the Cerec InLAB unit [Cerec InLAB, Diamond D64 (64 μm); Sirona, Germany] and then sintered to full density in a high-temperature furnace (Sintramat, Ivoclar Vivadent, Schaan, Liechtenstein; 1500°C for 30 min) according to the manufacturer's instructions. The top-surface side of the Y-TZP plate was ground flat and parallel with 600-grit (30 μm) water-cooled resin bond diamond disks to a thickness of 0.5 mm, by means of a grinding machine (Ecomet 4, Buehler, Lake Bluff, IL, USA). This surface was subsequently mirror-polished with successive grits to a 1-μm finish.

The cementation surfaces of the Y-TZP specimens were subjected to different surface treatments before adhesive cementation. In Test Group Ground samples (n = 24), the surfaces of the Y-TZP plates were ground with 600-grit (30 μm) water-cooled resin bonded diamond disks. In Test Group Alumina-abraded samples (n = 24), the intaglio surface was abraded with 50 μm Al<sub>2</sub>O<sub>3</sub> at a pressure of 0.5 MPa for 5 sec at a distance of 10 mm. In Control Group Machined samples (n = 24), specimens remained untreated, with the characteristic machined and then sintered surfaces. In Groups Ground and Machined, the intaglio surface was treated with NaOH (0.1 molar) for 10 sec, rinsed, and dried, to promote stable adhesion to a phosphate-based primer. Prior to cementation, a metal primer (Alloy Primer, Kuraray, Tokyo, Japan) was applied in all groups. Resin composite blocks (RCBs) (12 x 12 x 4 mm) (Z-100, 3M-ESPE, St. Paul, MN, USA) were aged in water for 60 days to allow for hygroscopic expansion. RCBs were sandblasted with 50 μm Al<sub>2</sub>O<sub>3</sub> (0.5 MPa for 5 sec at a distance of 10 mm) and ultrasonically cleaned. To obtain a defined resin cement thickness, we placed plastic foil spacers of 50-μm thickness on 2 opposite corners of the RCB squares. The primed ceramic surfaces were bonded to the RCBs with resin cement (Panavia 21, Kuraray, Osaka, Japan) according to the manufacturer's instruction. To simulate *in vivo* conditions of the oral cavity, we aged bonded specimens in water for 10 days prior to fatigue-testing.

Single-load-to-failure (SLF) Hertzian contact testing (n = 3) was performed with a universal mechanical testing machine (Instron 5566, Instron Co., Canton, MA, USA). The load was applied through a tungsten carbide (WC) ball (r = 3.18 mm) at a crosshead speed of 1.0 mm/min until fracture occurred. The resulting mean value permitted the establishment of profiles for the subsequent step-stress fatigue testing.

### Fatigue Tests

Twenty-one samples from each group were exposed to uni-axial mouth-motion step-stress fatigue in an electrodynamic testing machine (ELF 3300, EnduraTEC Systems Corporation, Minnetonka, MN, USA). Cyclic fatigue load was applied with a spherical WC indenter (r = 3.18 mm) at 1.5-2 Hz in water. The step-stress test method (overstress acceleration) applied several

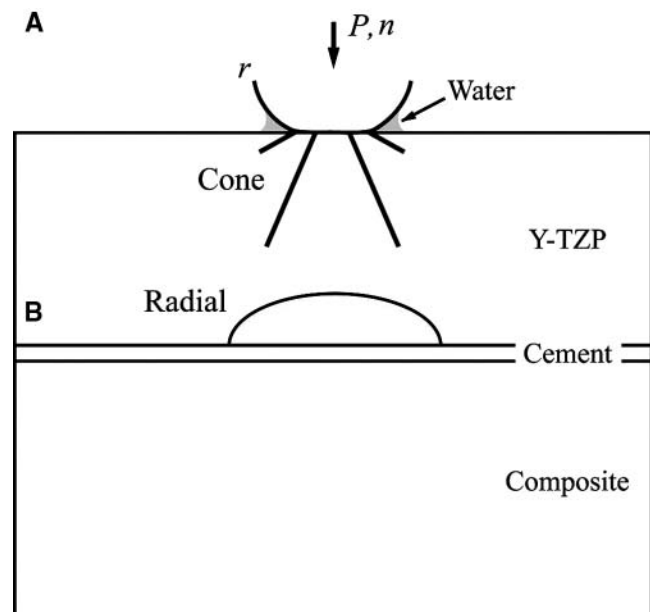


**Figure 1.** Schematic diagram of crack geometry for uni-axial cyclic contact loading with a WC spherical indenter ( $r = 3.18$  mm) on monolithic Y-TZP ceramic bonded to dentin-like composite. **(a)** Formation of deep penetrating cone crack on load application site. **(b)** Formation of flexural radial crack on cementation surface site.

stress levels sequentially for a predetermined number of cycles at each stress level (Kim *et al.*, 2007). Specimens were distributed across three different step-stress profiles in a ratio of 4:2:1, from the least aggressive to the most aggressive loading profile. At the end of each period of load-cycling, samples were inspected for failure with a polarized light stereomicroscope (MZ APO, Leica, Wetzlar, Germany) and a 3-D specular reflection microscope (Model H-160, Edge Scientific Co., Honolulu, HI, USA). Failure modes were categorized as surface cone fracture and/or bottom surface radial fracture. Failed specimens were embedded in epoxy resin (EpoFix, Struers, Ballerup, Denmark), and cross-sections were inspected (by stereomicroscopy) to confirm the failure mode. The fatigue data were analyzed by reliability software (Alta 7 Pro, Reliasoft, Tucson, AZ, USA) dependent on the verification of failure modes. The Weibull distribution was applied, and reliability was calculated for a mission of 100,000 cycles at 200-N load. We compared Weibull reliabilities for the overlap of their two-sided confidence bounds (CB) at the 90% level to determine if datasets were different.

### XRD Analysis

The amount of the monoclinic phase after various surface treatments was determined with an x-ray diffractometer (XRD) equipped with Cu-K $\alpha$  radiation (Philips X'Pert X-ray Diffractometer, Philips Analytical Inc., Natick, MA, USA). XRD spectra were collected over a  $2\theta$  range between 27° and 33° at a scan speed of 1°/min and a step size of 0.02°. The monoclinic phase fraction was calculated by the Garvie-Nicholson method (Garvie and Nicholson, 1972).

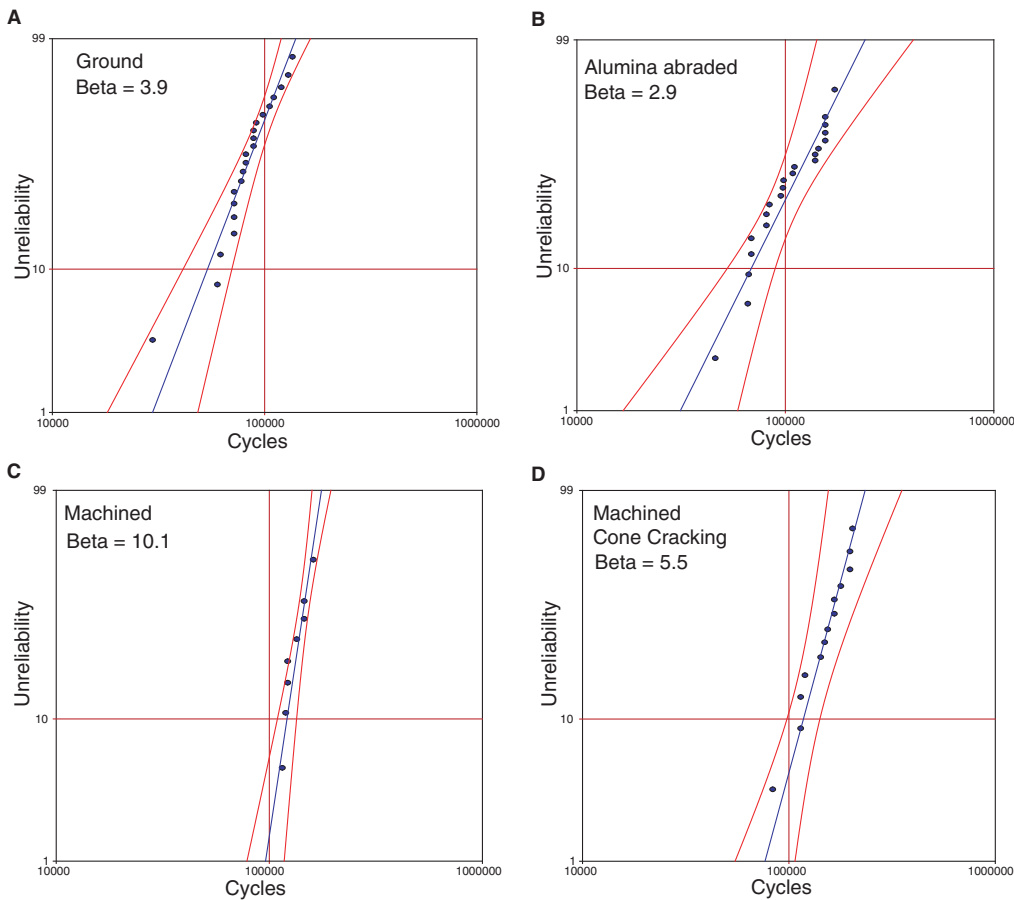


**Figure 2.** Use-level Weibull unreliability plots for radial cracking (**A-C**) and surface cone cracking (**D**) in a Y-TZP ceramic core/composite substrate system as a function of time (cycles) at 200-N load with two-sided 90% confidence bounds. Datapoints (blue points) are experimental results of individual tests showing radial cracks. Two-sided confidence bounds at 90% are displayed as red lines. (A) Plot of 600-grit ground Y-TZP ceramic ( $n = 21$  specimens, 15 radial failures, and 6 by surface cracking or suspension), Weibull modulus,  $\beta = 3.9$ . (B) Plot of alumina-abraded Y-TZP ceramic ( $n = 21$  specimens, 19 radial fractures, and 2 by cone cracking), Weibull modulus,  $\beta = 2.9$ . (C) Plot of as-received (Machined) Y-TZP ceramic ( $n = 21$  specimens, 8 failed by radial fracture, Weibull modulus,  $\beta = 10.1$ ). (D) Use-level unreliability plot for cone cracking for Machined group [13 remaining specimens from (C), Weibull modulus,  $\beta = 5.5$ ] showing the competition between failure modes for the machined group.

## RESULTS

The single-load-to-failure mean value was  $328 \pm 7$  N for 600-grit ground (Group Ground),  $315 \pm 11$  N for alumina-abraded (Group Alumina-abraded), and  $446 \pm 84$  N for the as-received control samples (Group Machined). The step-stress-derived probability Weibull plots at 200-N load and 100,000 cycles are shown in Fig. 2. The calculated reliability with 90% confidence bounds of ground and alumina-abraded test specimens was comparable [0.41 Group Ground (confidence bounds, 0.56-0.25); 0.56 Group Alumina-abraded (confidence bounds 0.72-0.37)]. The fatigue reliability of control specimens [0.98 Group Machined (confidence bounds, 0.99-0.90)] was significantly higher, as indicated by non-overlap of the confidence bounds.

Sections of failed specimens revealed different fatigue failure modes induced by the different surface treatments. Radial cracks

developing from the pre-treated core cementation side formed the prevalent failure mode of ground (15 out of 21 specimens = 71%) and alumina-abraded (19 out of 21 specimens = 90%) specimens (Fig. 3A, B). As-received machined specimens failed mainly from contact-induced deep penetrating cone cracks (13 out of 21 specimens = 62%) (Fig. 3C), giving significantly higher 10% reliability; radial cracks developed at generally higher load levels (Fig. 2C).

The amounts of monoclinic zirconia detected by XRD on treated surfaces of the specimens were determined before and after aging in water for 10 days (Figs. 4A and 4B, respectively). No significant difference in XRD spectra was observed in specimens before and after the 10 days' aging in water. No phase transformation was revealed in as-received specimens [see spectrum (i) in Fig. 4]. Small amounts of monoclinic zirconia were observed in alumina-abraded ( $\sim 6$  wt%) [spectrum (ii)] and ground ( $\sim 3$  wt%) [spectrum (iii)] surfaces. Thus, the amount of compressive stress associated with the phase transformation was relatively small.

## DISCUSSION

Quantitative fractography of clinically failed Y-TZP crowns revealed that cracks initiated at the internal (cementation) surface in the occlusal region of the restorations, where the greatest tensile stress concentrates and/or damage accumulates during occlusion (Aboushelib *et al.*, 2008). Hence, radial fracture initiating from the cementation surface was considered as a key indicator in the present study on differently treated Y-TZP surfaces.

The hypothesis that post-sintering surface treatment affected the damage mode and fatigue behavior of zirconia was accepted. Cementation surface radial cracking was observed as the dominant failure mode in ground and alumina-abraded Y-TZP ceramic. Post-sintering surface damage due to grinding and alumina abrasion may introduce some form of *quasi*-plasticity accompanied by microcracks acting as fracture initiation sites.

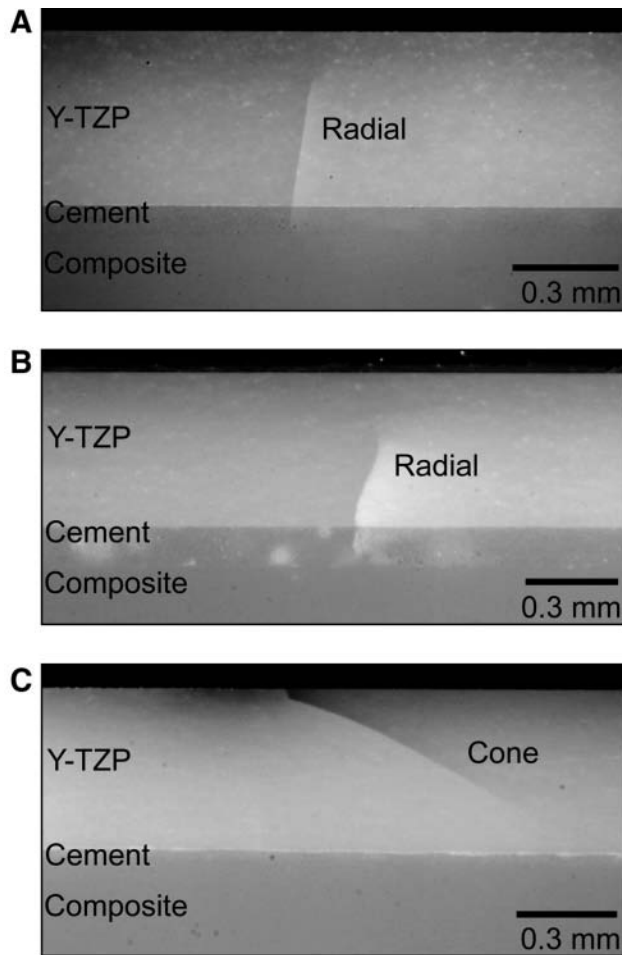


**Figure 3.** Section of failed Y-TZP flat-layer specimens after uni-axial mouth-motion cyclic loading with a WC spherical indenter ( $r = 3.18$  mm), indicating different failure modes, imaged with polarized light. **(A)** Cementation surface radial crack after 600-grit grinding at 225 N and 70 K cycles. **(B)** Cementation surface radial crack after alumina abrasion at 250 N and 80 K cycles. **(C)** Load surface cone crack of as-received Y-TZP ceramic at 550 N and 180 K cycles.

With mouth-motion fatigue loading, small defects such as microcracks tended to coalesce and grow until reaching a critical size, resulting in catastrophic failure from radial fracture. A previous study revealed that the damage induced by severe alumina abrasion not only occurred at the surface, but also extended to the subsurface region to a depth of  $\sim 4$   $\mu\text{m}$  (Zhang *et al.*, 2004). Microcracks with depths of 15  $\mu\text{m}$  after grinding have been reported in densely sintered Y-TZP (Luthardt *et al.*, 2004). These surface defects act as stress concentration sites, which magnify the applied stresses (Curtis *et al.*, 2006). Trace moisture has been shown to strongly exacerbate fatigue crack propagation by slow crack growth (Zhang *et al.*, 2004, 2006).

Since the condition of the cementation surface is likely a dominant factor in the long-term performance of Y-TZP ceramic, a baseline value for comparison needs to be defined. Under clinical circumstances, zirconia core ceramics contain different types of surface damage and flaws as a result of CAD/CAM milling procedures (Luthardt *et al.*, 2002). For some

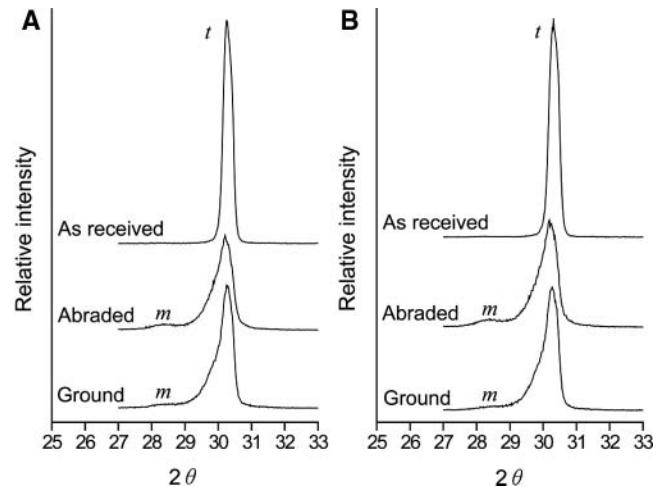


**Figure 4.** XRD spectrum of Y-TZP specimens **(a)** before and **(b)** after being subjected to 10 days' aging in water. Spectra were collected from as-received CAD/CAM, alumina-abraded, and ground ceramics. Low-level diffraction peaks due to monoclinic  $\text{ZrO}_2$  ( $m$ ) were observed with alumina abrasion ( $\sim 6$  wt%) and grinding ( $\sim 3$  wt%). 100% tetragonal phase ( $t$ ) of as-received Y-TZP ceramic.

CAD/CAM systems, ceramics are machined in a partially sintered form and then fired to a fully dense form, whereas for others, the fully dense material is shaped. The CAD/CAM milling procedure for the present Y-TZP ceramic was executed before the final sintering. The as-received CAD/CAM-machined Y-TZP ceramic failed predominantly from contact-induced surface cone cracks. Cyclic loading resulted in Hertzian stresses in the near-contact region, leading to the formation of cone cracks. Subsequent loading drove cone cracks deep, which eventually propagated through the sample thickness. The crack initiation site of as-received Y-TZP ceramic was predominantly on the loading surface, indicating that the flaw density on the cementation surface was reduced when compared with that on ground and alumina-abraded samples. This can be attributed to the industrial fabrication of Y-TZP blanks by the manufacturer, ensuring tight processing and quality control. In addition, the sintering procedure after milling might have a healing effect on the surface damage caused by CAD/CAM machining (Wang *et al.*, 2008).

The failure behavior can be further explained and confirmed by the reliability findings. In failure by bottom surface radial cracking, the calculated reliability for a clinically relevant mission of a 200-N load and 100,000 cycles (DeLong and Douglas, 1991) is 41% for ground and 56% for alumina-abraded surfaces, compared with a 98% reliability for as-received Y-TZP core ceramic. The reliability degradation of ground surfaces is similar to that induced by alumina particle abrasion. It is important to note that the observed radial crack formation in ground and alumina-abraded ceramics occurred at stress levels that are considerably lower than those required for the as-received ceramic. Ground and alumina-abraded zirconia specimens showed a 5% probability of failure at  $\sim 45,000$  cycles under a 200-N load. As-received zirconia specimens revealed a 10% probability of failure at a significantly higher number of cycles ( $> 100,000$ ).

The higher Weibull modulus ( $> 10$ ) of the as-received Y-TZP ceramic characterizes the low inherent flaw density and high structural reliability compared with the significantly lower values obtained after post-sintering grinding (3.4) and alumina abrasion (2.9). These low Weibull moduli are indicative of substantial point-to-point variation in surface state, suggesting an increase in microcrack density within the damage layer. It has been reported that grinding and alumina abrasion introduced deep surface flaws which can act as stress concentrators and become strength-limiting factors if flaw length extends beyond the surface compressive layer (Luthardt *et al.*, 2002, 2004; Wang *et al.*, 2008).

However, several research groups have claimed increased flexural strength in Y-TZP (Sato *et al.*, 2008), due to phase transformation after grinding and alumina abrasion (Kosmac *et al.*, 1999, 2000; Guazzato *et al.*, 2005), but no study has been conducted to investigate bonded interfaces equilibrated in water as tested herein. Depending on the specific material microstructure and manufacturer processing regimes, grinding or alumina abrasion treatment can induce tetragonal to monoclinic phase transformation in Y-TZP (Kosmac *et al.*, 1999). Our XRD analysis revealed a small amount of transformation at the present post-sintering ground and alumina-abraded Y-TZP surfaces. In addition, broadening of the (111) tetragonal Y-TZP peak following post-sintering grinding and alumina abrasion indicates the introduction of surface strain. The transformed monoclinic phase and surface strain create a layer of compressive stresses that could inhibit microcrack extension, thus serving to strengthen the material. However, any temporary beneficial effect induced by different surface treatment methods can be counteracted by heat treatment associated with the application of a porcelain veneer and fatigue-related crack growth phenomena (Guazzato *et al.*, 2005). Thus, single-cycle strength testing could greatly overestimate stress-bearing capacity (Teixeira *et al.*, 2007). Finally, porcelain-veneered Y-TZP layer structures or full crowns tested in a similar manner would be expected to fail by cone cracks before core failure (Kim *et al.*, 2008; Coelho *et al.*, 2009). Our test method allowed cementation surface treatment effects to be explored. Clinically, Y-TZP frameworks can be exposed to direct load application in certain circumstances, for either design [resin-bonded (Komine and Tomic, 2005) and inlay-retained FPDs (Wolfart and Kern, 2006)] or wear/occlusal adjustment-related (Aboushelib *et al.*, 2008) reasons. The conclusions drawn from the present study may be limited to the Y-TZP material tested.

## ACKNOWLEDGMENTS

This work was supported by Ivoclar Vivadent and by NIH (NIDCR 1R01 DE017925, P01 DE10976) and NSF (CMMI-0758530). Preliminary work was presented at the AADR Annual Meeting in Dallas, TX, USA, April, 2008.

## REFERENCES

- Aboushelib MN, Feilzer AJ, Kleverlaan CJ (2008). Bridging the gap between clinical failure and laboratory fracture strength tests using a fractographic approach. *Dent Mater* 25:383-391.
- Christel P, Meunier A, Heller M, Torre JP, Peille CN (1989). Mechanical properties and short-term *in-vivo* evaluation of yttrium-oxide-partially-stabilized zirconia. *J Biomed Mater Res* 23:45-61.
- Coelho PG, Bonfante EA, Silva NR, Rekow ED, Thompson VP (2009). Laboratory simulation of Y-TZP crown clinical failures. *J Dent Res* 86:142-146.
- Curtis AR, Wright AJ, Fleming GJ (2006). The influence of surface modification techniques on the performance of a Y-TZP dental ceramic. *J Dent* 34:195-206.
- DeLong R, Douglas WH (1991). An artificial oral environment for testing dental materials. *IEEE Trans Biomed Eng* 38:339-345.
- Filser F, Kocher P, Weibel F, Luthy H, Scharer P, Gauckler LJ (2001). Reliability and strength of all-ceramic dental restorations fabricated by direct ceramic machining (DCM). *Int J Comput Dent* 4:89-106.
- Garvie RC, Nicholson PS (1972). Phase analysis in zirconia systems. *J Am Ceram Soc* 55:303-305.
- Guazzato M, Quach L, Albakry M, Swain MV (2005). Influence of surface and heat treatments on the flexural strength of Y-TZP dental ceramic. *J Dent* 33:9-18.
- Kim B, Zhang Y, Pines M, Thompson VP (2007). Fracture of porcelain-veneered structures in fatigue. *J Dent Res* 86:142-146.
- Kim JW, Kim JH, Janal MN, Zhang Y (2008). Damage maps of veneered zirconia under simulated mastication. *J Dent Res* 87:1127-1132.
- Komine F, Tomic M (2005). A single-retainer zirconium dioxide ceramic resin-bonded fixed partial denture for single tooth replacement: a clinical report. *J Oral Sci* 47:139-142.
- Kosmac T, Oblak C, Jevnikar P, Funduk N, Marion L (1999). The effect of surface grinding and sandblasting on flexural strength and reliability of Y-TZP zirconia ceramic. *Dent Mater* 15:426-433.
- Kosmac T, Oblak C, Jevnikar P, Funduk N, Marion L (2000). Strength and reliability of surface treated Y-TZP dental ceramics. *J Biomed Mater Res* 53:304-313.
- Lawn BR, Deng Y, Thompson VP (2001). Use of contact testing in the characterization and design of all-ceramic crownlike layer structures: a review. *J Prosthet Dent* 86:495-510.
- Luthardt RG, Holzhueter M, Sandkuhl O, Herold V, Schnapp JD, Kuhlisch E, *et al.* (2002). Reliability and properties of ground Y-TZP-zirconia ceramics. *J Dent Res* 81:487-491.
- Luthardt RG, Holzhueter MS, Rudolph H, Herold V, Walter MH (2004). CAD/CAM-machining effects on Y-TZP zirconia. *Dent Mater* 20:655-662.
- Sailer I, Feher A, Filser F, Gauckler LJ, Luthy H, Hämmerle CH (2007). Five-year clinical results of zirconia frameworks for posterior fixed partial dentures. *Int J Prosthodont* 20:383-388.
- Sato H, Yamada K, Pezzotti G, Nawa M, Ban S (2008). Mechanical properties of dental zirconia ceramics changed with sandblasting and heat treatment. *Dent Mater J* 27:408-414.
- Taskonak B, Yan J, Mecholsky JJ Jr, Sertgoz A, Kocak A (2008). Fractographic analyses of zirconia-based fixed partial dentures. *Dent Mater* 24:1077-1082.
- Teixeira EC, Piascik JR, Stoner BR, Thompson JY (2007). Dynamic fatigue and strength characterization of three ceramic materials. *J Mater Sci Mater Med* 18:1219-1224.
- Tinschert J, Zwez D, Marx R, Anusavice KJ (2000). Structural reliability of alumina-, feldspar-, leucite-, mica- and zirconia-based ceramics. *J Dent* 28:529-535.
- Wang H, Aboushelib MN, Feilzer AJ (2008). Strength influencing variables on CAD/CAM zirconia frameworks. *Dent Mater* 24:633-638.
- Wolfart S, Kern M (2006). A new design for all-ceramic inlay-retained fixed partial dentures: a report of 2 cases. *Quintessence Int* 37:27-33.
- Wolfart S, Lehmann F, Wolfart M, Kern M (2007). Durability of the resin bond strength to zirconia ceramic after using different surface conditioning methods. *Dent Mater* 23:45-50.
- Zhang Y, Lawn BR, Rekow ED, Thompson VP (2004). Effect of sandblasting on the long-term performance of dental ceramics. *J Biomed Mater Res B Appl Biomater* 71:381-386.
- Zhang Y, Lawn BR, Malament KA, Van Thompson P, Rekow ED (2006). Damage accumulation and fatigue life of particle-abraded ceramics. *Int J Prosthodont* 19:442-448.